Commun Nonlinear Sci Numer Simulat 17 (2012) 2447–2462

Contents lists available at SciVerse ScienceDirect

Commun Nonlinear Sci Numer Simulat

journal homepage: www.elsevier.com/locate/cnsns

Mixed convection flow of couple stress fluid between parallel vertical plates with Hall and Ion-slip effects

D. Srinivasacharya *, K. Kaladhar

Department of Mathematics, National Institute of Technology, Warangal 506 004, India

ARTICLE INFO

Article history:
Received 26 January 2011
Received in revised form 2 July 2011
Accepted 9 October 2011
Available online 21 October 2011

Keywords:
Mixed convection
Couple stress fluid
MHD
Hall and Ion-slip effects
HAM

ABSTRACT

An analysis is presented to investigate the Hall and Ion-slip effects on fully developed electrically conducting couple stress fluid flow between vertical parallel plates in the presence of a temperature dependent heat source. The governing non-linear partial differential equations are transformed into a system of ordinary differential equations using similarity transformations and then solved using homotopy analysis method (HAM). The effects of the magnetic parameter, Hall parameter, Ion-slip parameter and couple stress fluid parameter on velocity and temperature are discussed and shown graphically.

1. Introduction

Heat transfer in free and mixed convection in vertical channel has been the focus of extensive investigation for many decades due to its wide range of applications in the design of cooling systems for electronic devices and in the field of solar energy collection, etc. Heat exchanger technology involves convective flows in vertical channels. Several researchers have studied analytically and mostly numerically the problem of mixed convection heat transfer and fluid flow between vertical parallel plates. Aung and Worku [1] presented an exact solution for fully developed mixed convection in a parallel-plate vertical channel and compared it to their numerical results for developing flow at great distances from the channel entry. Cheng et al. [2] have investigated the problem of flow reversal and heat transfer of fully developed mixed convection in vertical channels. Analytical solution for fully developed mixed convection between parallel vertical plates with heat and mass transfer presented by Boulama and Galanis [3]. Rao and Narasimham [4] have considered the laminar conjugate mixed convection in a vertical channel with heat generating components. Ameni et al. [5] investigated numerically the mixed convection in a vertical heated channel.

A combined free and forced convection flow of an electrically conducting fluid in a channel in the presence of a transverse magnetic field is of special technical significance because of its frequent occurrence in many industrial applications such as geothermal reservoirs, cooling of nuclear reactors, thermal insulation, petroleum reservoirs, etc. This type of problem also arises in electronic packages, microelectronic devices during their operations. In recent years, several convection heat transfer and fluid flow problems have received new attention within the more general context of magnetohydrodynamics (MHD). Several investigators have extended many of the available convection heat transfer and fluid flow problems to include the effects of magnetic fields for those cases when the fluid is electrically conducting. Alireza and Sahai [6] studied the effect of temperature-dependent transport properties on the developing MHD flow and heat transfer in a parallel-plate channel

* Corresponding author.
E-mail addresses: dsc@nitw.ac.in, dsrinivasacharya@yahoo.com (D. Srinivasacharya).

1007-5704/$ - see front matter © 2011 Elsevier B.V. All rights reserved.
doi:10.1016/j.cnsns.2011.10.006

whose walls were held at constant and equal temperatures. Umavathi and Malashetty [7] analyzed the problem of combined free and forced convective magnetohydrodynamic flow in a vertical channel by taking into account the effect of viscous and ohmic dissipations. Barletta and Ceilla [8] obtained the solutions both analytically by a power series method and numerically for Mixed convection MHD flow in a vertical channel by taking into account the effects of Joule heating and viscous dissipation. Recently Prathap Kumar et al. [9] studied mixed convection of composite porous medium in a vertical channel with a symmetric wall heating conditions.

In most of the MHD flow problems, the Hall and Ion-slip terms in Ohms law were ignored. However, in the presence of strong magnetic field, the influence of Hall current and Ion-slip are important. Tani [10] studied the Hall effects on the steady motion of electrically conducting viscous fluid in channels. Hall and Ion-slip effects on MHD Couette flow with heat transfer have been considered by Soundelgekar et al. [11]. Attia [12] considered the steady Couette flow of an electrically conducting viscous incompressible fluid between two parallel horizontal non-conducting porous plates with heat transfer, taking the Ion-slip into consideration.

During recent years the study of convection heat and mass transfer in non-Newtonian fluids has received much attention and this is because the traditional Newtonian fluids cannot precisely describe the characteristics of the real fluids. A theoretical study of the fully developed mixed convection flow of a micropolar fluid in a parallel plate vertical channel with an asymmetric wall temperature distribution has been presented by Ali and Chamkha [13]. Ziabakhsh and Domairry [14] have obtained the solution for natural convection of the Rivlin–Ericksen fluid of grade three between two infinite parallel vertical flat plates. Sajid et al. [15] studied fully developed mixed convection flow of a viscoelastic fluid between permeable parallel vertical walls using HAM. Some of the published papers on different non-Newtonian fluids, such as Brian [16], Kaloni and Siddiqui [17], Rudraiah et al. [18], Kaloni and Lou [19], Hayat et al. [20–22], Fetecau et al. [23–25]. In addition, progress has been considerably made in the study heat and mass transfer in magneto hydrodynamic flow of non-Newtonian fluids due to its application in many devices, like the MHD power generator, aerodynamics heating, electrostatic precipitation and Hall accelerator etc. Different models have been proposed to explain the behavior of non-Newtonian fluids. Among these, couple stress fluids introduced by Stokes [26] have distinct features, such as the presence of couple stresses, body couples and non-symmetric stress tensor. The couple stress fluid theory presents models for fluids whose microstructure is mechanically significant. The effect of very small microstructure in a fluid can be felt if the characteristic geometric dimension of the problem considered is of the same order of magnitude as the size of the microstructure. The main feature of couple stresses is to introduce a size dependent effect. Classical continuum mechanics neglects the size effect of material particles within the continua. This is consistent with ignoring the rotational interaction among particles, which results in symmetry of the force-stress tensor. However, in some important cases such as fluid flow with suspended particles, this cannot be true and a size dependent couple-stress theory is needed. The spin field due to microrotation of freely suspended particles set up an antisymetric stress, known as couple-stress, and thus forming couple-stress fluid. These fluids are capable of describing various types of lubricants, blood, suspension fluids etc. The study of couple-stress fluids has applications in a number of processes that occur in industry such as the extrusion of polymer fluids, solidification of liquid crystals, cooling of metallic plate in a bath, and colloidal solutions etc. Stokes [26] discussed the hydromagnetic steady flow of a fluid with couple stress effects. A review of couple stress (polar) fluid dynamics was reported by Stokes [27].

The homotopy analysis method [28] was first proposed by Liao in 1992, is one of the most efficient methods in solving different types of nonlinear equations such as coupled, decoupled, homogeneous and non-homogeneous. Also, HAM provides us a great freedom to choose different base functions to express solutions of a nonlinear problem [29]. The application of the homotopy analysis method (HAM) in engineering problems is highly considered by scientists, because HAM provides us with a convenient way to control the convergence of approximation series, which is a fundamental qualitative difference in analysis between HAM and other methods. Later Liao [30] presented an optimal homotopy analysis approach for strongly nonlinear differential equations. HAM is used to get analytic approximate solutions for heat transfer of a micropolar fluid through a porous medium with radiation by Rashidi et al. [31]. Si et al. [32] accessed HAM solutions for the asymmetric laminar flow in a porous channel with expanding or contracting walls. Recent developments of HAM, like convergence of HAM solution, Optimality of convergence control parameter discussed by Turkyilmazoglu [33,34].

In this paper, we have investigated the Hall and Ion-slip effects on steady mixed convective heat transfer flow between two vertical parallel plates in couple stress fluid. The homotopy analysis method is employed to solve the governing nonlinear equations. Convergence of the derived series solution is analyzed. The behavior of emerging flow parameters on the velocity and temperature is discussed.

2. Mathematical formulation

Consider an incompressible electrically conducting couple stress fluid flow between two vertical parallel plates distance $2d$ apart. Choose the coordinate system such that x-axis be taken along vertically upward direction through the central line of the channel, y is perpendicular to the plates and the two plates are infinitely extended in the direction of x and z. The plates of the channel are at $y = \pm d$. The flow is subjected to a uniform magnetic field perpendicular to the flow direction with the Hall and Ion-slip effects. The effect of Hall and Ion-slip current gives rise to force in the z-direction, which induces a cross flow in that direction and hence the flow becomes three dimensional. Assume that the flow is steady and the magnetic Reynolds number is very small so that the induced magnetic field can be neglected in comparison with the applied magnetic

field. Further, assume that all the fluid properties are constant except the density in the buoyancy term of the balance of momentum equation. With the above assumptions, the equations governing the steady flow of an incompressible couple stress fluid, under usual MHD approximations are

$$\frac{\partial v}{\partial y} = 0, \tag{1}$$

$$\rho v \frac{\partial u}{\partial y} = -\frac{\partial p}{\partial x} + \mu \frac{\partial^2 u}{\partial y^2} - \eta_1 \frac{\partial^4 u}{\partial y^4} + \rho g \beta_T (T - T_0) - \frac{\sigma B_0^2}{\alpha_e^2 + \beta_h^2}(\alpha_e u + \beta_h w), \tag{2}$$

$$\rho v \frac{\partial w}{\partial y} = \mu \frac{\partial^2 w}{\partial y^2} - \eta_1 \frac{\partial^4 w}{\partial y^4} + \frac{\sigma B_0^2}{\alpha_e^2 + \beta_h^2}(\beta_h u - \alpha_e w), \tag{3}$$

$$\rho C_p v \frac{\partial T}{\partial y} = K_f \frac{\partial^2 T}{\partial y^2} + 2\mu \left[\left(\frac{\partial u}{\partial y} \right)^2 + \left(\frac{\partial w}{\partial y} \right)^2 \right] + \eta_1 \left[\left(\frac{\partial^2 u}{\partial y^2} \right)^2 + \left(\frac{\partial^2 w}{\partial y^2} \right)^2 \right] + \gamma_0 v (T - T_0), \tag{4}$$

where u, v, w are respectively the x-, y- and z-components of the velocity, p is the pressure, ρ is the density, C_p is the specific heat, μ is the coefficient of viscosity, β_h is the Hall parameter, β_i is the Ion-slip parameter, $\alpha_e = 1 + \beta_h \beta_i$, β_T is the coefficient of thermal expansion, K_f is the coefficient of thermal conductivity, η_1 is the couple stress fluid parameter, T_0 is the temperature in hydrostatic state, γ_0 is the constant of proportionality and $\gamma_0 v(T - T_0)$ is the amount of heat generated per unit volume in unit time, which is assumed to be a linear function of temperature. From Eq. (1), we observe that the velocity component v is constant i.e. $v = v_0$.

The boundary conditions are given by

$$u = 0, \quad w = 0, \quad \text{at} \quad y = \pm d, \tag{5a}$$

$$u_{yy} = 0, \quad w_{yy} = 0 \quad \text{at} \quad y = \pm d, \tag{5b}$$

$$T = T_1, \quad \text{at} \quad y = -d, \quad T = T_2, \quad \text{at} \quad y = d. \tag{5c}$$

The boundary condition (5a) corresponds to the classical no-slip condition from viscous fluid dynamics. The boundary condition (5b) imply that the couple stresses are zero at the plate surfaces.

Introducing the following similarity transformations

$$y = \eta d, \quad u = u_0 U, \quad w = u_0 W, \quad T - T_0 = (T_2 - T_0)\theta \tag{6}$$

in Eqs. (2)–(4), we get the following nonlinear system of differential equations

$$\alpha^2 U^{(iv)} - U'' + RU' - \frac{Gr}{Re}\theta + \frac{Ha^2}{\alpha_e^2 + \beta_h^2}(\alpha_e U + \beta_h W) + A = 0, \tag{7}$$

$$\alpha^2 W^{(iv)} - W'' + RW' - \frac{Ha^2}{\alpha_e^2 + \beta_h^2}(\beta_h U - \alpha_e W) = 0, \tag{8}$$

$$\theta'' - RPr\theta' + 2Br\left[(U')^2 + (W')^2\right] + \alpha^2 Br\left[(U'')^2 + (W'')^2\right] + \gamma_1 RPr\theta = 0, \tag{9}$$

where primes denote differentiation with respect to η, $\alpha = \frac{1}{d}\sqrt{\frac{\eta_1}{\mu}}$ is the couple stress parameter, $Re = \frac{\rho u_0 d}{\mu}$ is the Reynolds number, $R = \frac{\rho v d}{\mu}$ is the suction/injuction parameter, $Pr = \frac{\mu C_p}{K_f}$ is the Prandtl number, $Ha = B_0 d\sqrt{\frac{\sigma}{\mu}}$ is the Hartmann number, $Gr = \frac{\rho^2 g \beta_T f_x d^3}{\mu^2}(T_2 - T_0)$ is the Grashof number, $Br = \frac{\mu u_0^2}{k_f (T_2 - T_0)}$ is the Brinkman number, $A = \frac{d^2}{\mu u_0}\frac{dp}{dx}$ is the constant pressure gradient and $\gamma_1 = \frac{\gamma_0 d}{\rho C_p}$ is the dimensionless vertical distance.

Boundary conditions (5) in terms of U,W, θ become

$$\begin{aligned} &U = 0, \quad W = 0, \quad U'' = 0, \quad W'' = 0, \quad \theta = r_T \quad \text{at} \quad \eta = -1, \\ &U = 0, \quad W = 0, \quad U'' = 0, \quad W'' = 0, \quad \theta = 1 \quad \text{at} \quad \eta = 1, \end{aligned} \tag{10}$$

where r_T is the wall temperature parameter.

3. The HAM solution of the problem

For HAM solutions, we choose the initial approximations of $U(\eta)$, $W(\eta)$ and $\theta(\eta)$ as follows:

$$U_0(\eta) = 0, \quad W_0(\eta) = 0, \quad \theta_0(\eta) = \frac{1}{2}(1 + r_T) + \frac{1}{2}(1 - r_T)\eta; \tag{11}$$

and choose the auxiliary linear operators:

$$L_1 = \frac{\partial^4}{\partial \eta^4}, \quad L_2 = \frac{\partial^2}{\partial \eta^2}, \tag{12}$$

such that

$$L_1(c_1 + c_2\eta + c_3\eta^2 + c_4\eta^3) = 0, \quad L_2(c_5 + c_6\eta) = 0. \tag{13}$$

where $c_i (i = 1,2,\ldots,6)$ are constants. Introducing non-zero auxiliary parameters h_1, h_2 and h_3, we develop the zeroth-order deformation problems as follow:

$$(1-p)L_1[U(\eta;p) - U_0(\eta)] = ph_1N_1[U(\eta;p)], \tag{14}$$
$$(1-p)L_1[W(\eta;p) - W_0(\eta)] = ph_2N_2[W(\eta;p)], \tag{15}$$
$$(1-p)L_2[\theta(\eta;p) - \theta_0(\eta)] = ph_3N_3[\theta(\eta;p)], \tag{16}$$

subject to the boundary conditions

$$\begin{aligned} &U(-1;p) = 0, \quad U(1;p) = 0, \quad U''(-1;p) = 0, \quad U''(1;p) = 0, \quad W(-1;p) = 0, \\ &W(1;p) = 0, \quad W''(-1;p) = 0, \quad W''(1;p) = 0, \quad \theta(-1;p) = r_T, \quad \theta(1;p) = 1, \end{aligned} \tag{17}$$

where $p \in [0,1]$ is the embedding parameter and the non-linear operators N_1, N_2 and N_3 are defined as:

$$N_1[U(\eta,p),W(\eta,p),\theta(\eta,p)] = \alpha^2 U^{(iv)} - U'' + RU' - \frac{Gr}{Re}\theta + \frac{Ha^2}{\alpha_e^2 + \beta_h^2}(\alpha_e U + \beta_h W) + A, \tag{18}$$

$$N_2[U(\eta,p),W(\eta,p),\theta(\eta,p)] = \alpha^2 W^{(iv)} - W'' + RW' - \frac{Ha^2}{\alpha_e^2 + \beta_h^2}(\beta_h U - \alpha_e W), \tag{19}$$

$$\begin{aligned} N_3[U(\eta,p),W(\eta,p),\theta(\eta,p)] &= \theta''(\eta,p) - RPr\theta'(\eta,p) + \gamma_1 RPr\theta + 2Br\left[(U'(\eta,p))^2 + (W'(\eta,p))^2\right] \\ &\quad + \alpha^2 Br[(U''(\eta,p))^2 + (W''(\eta,p))^2]. \end{aligned} \tag{20}$$

For $p = 0$, we have the initial guess approximations

$$U(\eta;0) = U_0(\eta), \quad W(\eta;0) = W_0(\eta), \quad \theta(\eta;0) = \theta_0(\eta). \tag{21}$$

When $p = 1$, Eqs. (14)–(16) are same as (7)–(9) respectively, therefore at $p = 1$ we get the final solutions

$$U(\eta;1) = U(\eta), \quad W(\eta;1) = W(\eta) \quad \theta(\eta;1) = \theta(\eta). \tag{22}$$

Hence the process of giving an increment to p from 0 to 1 is the process of $U(\eta;p)$ varying continuously from the initial guess $U_0(\eta)$ to the final solution $U(\eta)$ (similar for $W(\eta,p)$ and $\theta(\eta,p)$). This kind of continuous variation is called deformation in topology so that we call system Eqs. (14)–(17), the zeroth-order deformation equation. Next, the mth-order deformation equations follow as

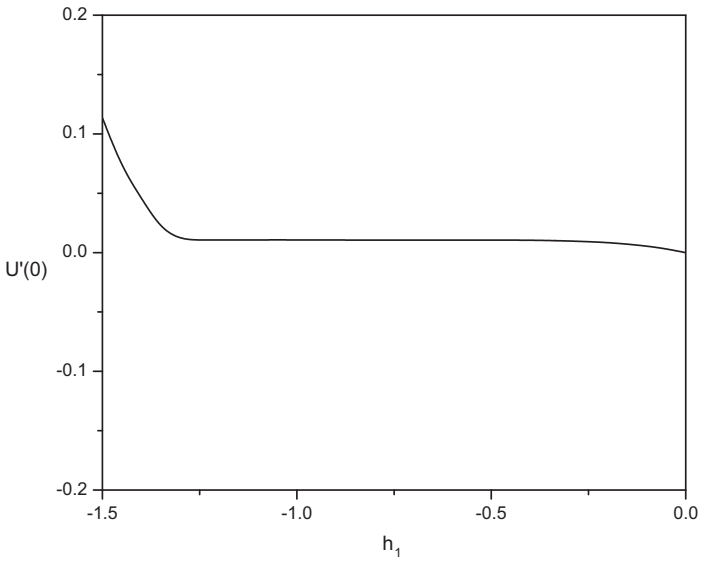

Fig. 1. h curve for $U(\eta)$ at $\beta_h = 2$, $\beta_i = 2$, $\alpha = 0.5$, $Ha = 2$.

$$L_1[U_m(\eta) - \chi_m U_{m-1}(\eta)] = h_1 R_m^U(\eta), \tag{23}$$

$$L_1[W_m(\eta) - \chi_m W_{m-1}(\eta)] = h_2 R_m^W(\eta), \tag{24}$$

$$L_2[\theta_m(\eta) - \chi_m \theta_{m-1}(\eta)] = h_3 R_m^\theta(\eta), \tag{25}$$

with the boundary conditions

$$\begin{aligned} &U_m(-1) = 0, \quad U_m(1) = 0, \quad U_m''(-1) = 0, \quad U_m''(1) = 0, \quad W_m(-1) = 0, \\ &W_m(1) = 0, \quad W_m''(-1) = 0, \quad W_m''(1) = 0, \quad \theta_m(-1) = 0, \quad \theta_m(1) = 0, \end{aligned} \tag{26}$$

where

$$R_m^U(\eta) = \alpha^2 U^{(iv)} - U'' + RU' - \frac{Gr}{Re}\theta + \frac{Ha^2}{\alpha_e^2 + \beta_h^2}(\alpha_e U + \beta_h W) + A(1 - \chi_m), \tag{27}$$

$$R_m^W(\eta) = \alpha^2 W^{(iv)} - W'' + RW' - \frac{Ha^2}{\alpha_e^2 + \beta_h^2}(\beta_h U - \alpha_e W), \tag{28}$$

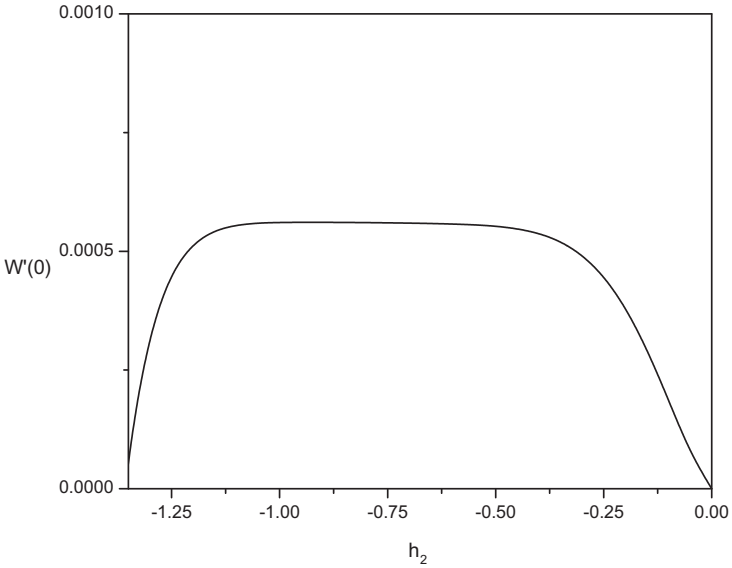

Fig. 2. h curve for $W(\eta)$ at $\beta_h = 2$, $\beta_i = 2$, $\alpha = 0.5$, $Ha = 2$.

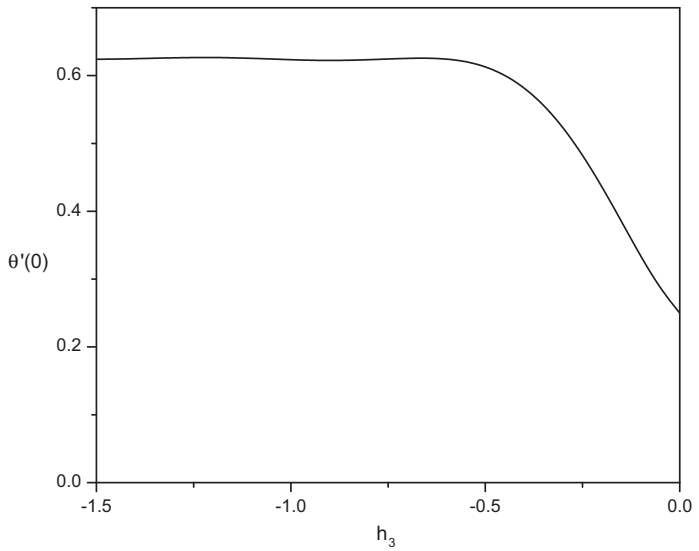

Fig. 3. h curve for $\theta(\eta)$ at $\beta_h = 2$, $\beta_i = 2$, $\alpha = 0.5$, $Ha = 2$.

$$R^{\theta}_m(\eta) = \theta'' - RPr\theta' + 2Br\left[\sum_{n=0}^{m-1}\left(U'_{m-1-n}U'_n + W'_{m-1-n}W'_n\right)\right] + \alpha^2 Br\left[\sum_{n=0}^{m-1}\left(U''_{m-1-n}U''_n + W''_{m-1-n}W''_n\right)\right] + \gamma_1 RPr\theta \tag{29}$$

and, for m being integer

$$\begin{aligned}\chi_m &= 0 \quad \text{for} \quad m \leqslant 1\\ &= 1 \quad \text{for} \quad m > 1\end{aligned} \tag{30}$$

The initial guess approximations $U_0(\eta)$, $W_0(\eta)$ and $\theta_0(\eta)$, the linear operators L_1, L_2 and the auxiliary parameters h_1,h_2 and h_3 are assumed to be selected such that Eqs. (14)–(17) have solution at each point $p \in [0,1]$ and also with the help of Taylors series and due to Eq. (21) $U(\eta;p)$, $W(\eta;p)$ and $\theta(\eta;p)$ can be expressed as

Table 1
Optimal value of h_1 at different order of approximations.

Order	Optimal of h_1	Minimum of E_m
10	−1.04	9.76×10^{-5}
15	−1.02	1.06×10^{-6}
20	−1.02	5.07×10^{-7}

Table 2
Optimal value of h_2 at different order of approximations.

Order	Optimal of h_2	Minimum of E_m
10	−0.96	1.98×10^{-7}
15	−0.99	4.49×10^{-8}
20	−0.99	4.75×10^{-9}

Table 3
Optimal value of h_3 at different order of approximations.

Order	Optimal of h_3	Minimum of E_m
10	−0.96	9.77×10^{-5}
15	−0.98	3.58×10^{-6}
20	−0.98	9.23×10^{-8}

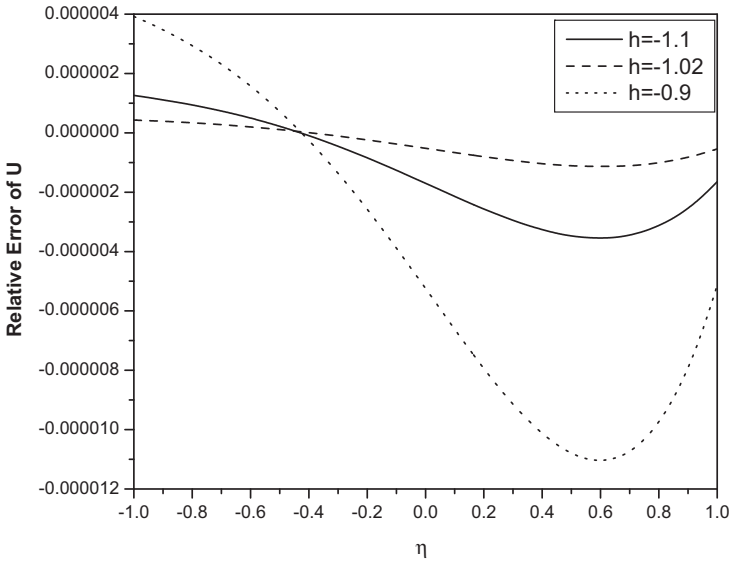

Fig. 4. Relative Error of $U(\eta)$ when $\beta_h = 2$, $\beta_i = 2$, $\alpha = 0.5$, $Ha = 2$.

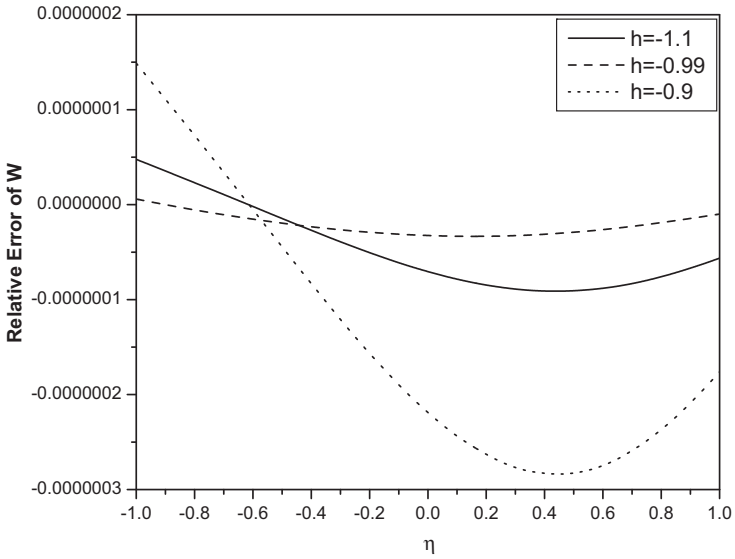

Fig. 5. Relative Error of $W(\eta)$ when $\beta_h = 2$, $\beta_i = 2$, $\alpha = 0.5$, $Ha = 2$.

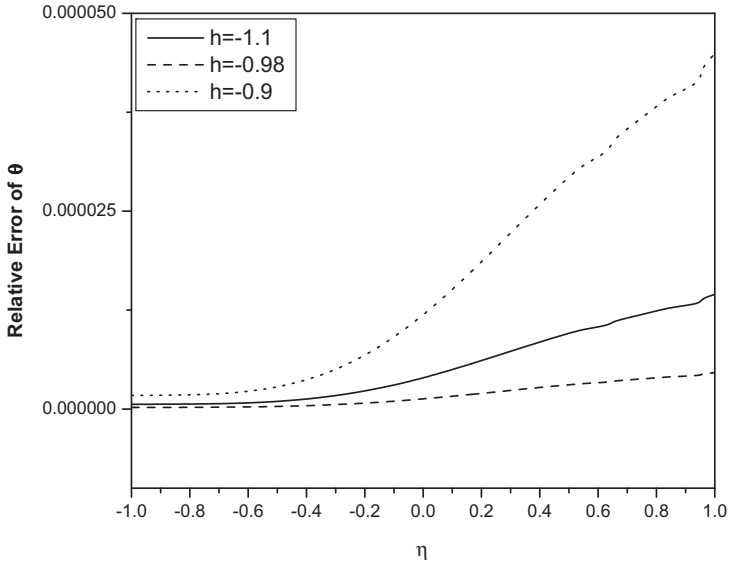

Fig. 6. Relative Error of $\theta(\eta)$ when $\beta_h = 2$, $\beta_i = 2$, $\alpha = 0.5$, $Ha = 2$.

Table 4
Convergence of HAM solutions for different order of approximations.

Order	$U(0)$	$W(0)$	$\theta(0)$
1	0.25625	0	1.86
5	0.266892314450323	0.0556513580716558	2.11301459157974
10	0.268922610628038	0.0547091691168198	2.13760247150632
15	0.268624397816504	0.0547282266072091	2.13823334196944
20	0.268624368904798	0.0547282179662947	2.13823318126976
30	0.268624368512822	0.0547282121359142	2.13823315212266
40	0.268624368431322	0.0547282121235081	2.13823315071245
50	0.268624368430807	0.0547282121227252	2.13823315070315

$$U(\eta;p) = U_0(\eta) + \sum_{m=1}^{\infty} U_m(\eta)p^m, \tag{31}$$

$$W(\eta;p) = W_0(\eta) + \sum_{m=1}^{\infty} W_m(\eta)p^m, \tag{32}$$

$$\theta(\eta;p) = \theta_0(\eta) + \sum_{m=1}^{\infty} \theta_m(\eta)p^m \tag{33}$$

in which h_1, h_2 and h_3 are choosen in such a way that the series (31)–(33) are convergent at $p = 1$. Therefore we have from (22) that

$$U(\eta) = U_0(\eta) + \sum_{m=1}^{\infty} U_m(\eta), \tag{34}$$

$$W(\eta) = W_0(\eta) + \sum_{m=1}^{\infty} W_m(\eta), \tag{35}$$

$$\theta(\eta) = \theta_0(\eta) + \sum_{m=1}^{\infty} \theta_m(\eta) \tag{36}$$

for which we presume that the initial guesses to U, W and θ the auxiliary linear operators L and the non-zero auxiliary parameters h_1, h_2 and h_3 are so properly selected that the deformation $U(\eta,p)$, $W(\eta,p)$ and $\theta(\eta,p)$ are smooth enough and their m*th*-order derivatives with respect to p in Eqs. (34)–(36) exist and are given respectively by $U_m(\eta) = \frac{1}{m!}\frac{\partial^m U(\eta;p)}{\partial p^m}\Big|_{p=0}$, $W_m(\eta) = \frac{1}{m!}\frac{\partial^m W(\eta;p)}{\partial p^m}\Big|_{p=0}$, $\theta_m(\eta) = \frac{1}{m!}\frac{\partial^m \theta(\eta;p)}{\partial p^m}\Big|_{p=0}$. It is clear that the convergence of Taylor series at $p = 1$ is a prior assumption, whose justification is provided via a theorem [34], so that the system in (34)–(36) holds true. The formulae in (34)–(36) provide us with a direct relationship between the initial guesses and the exact solutions. All the effects of interaction of the magnetic field as well as of the heat transfer, Hall and Ion effects and couple stress flow field can be studied from the exact formulas (34)–(36). Moreover, a special emphasize should be placed here that the mth-order deformation system (23)–(26) is a linear differential equation system with the auxiliary linear operators L whose fundamental solution is known.

4. Convergence of the HAM solution

The expressions for U, W and θcontain the auxiliary parameters h_1, h_2 and h_3. As pointed out by Liao [28], the convergence and the rate of approximation for the HAM solution strongly depend on the values of auxiliary parameter h. For this purpose, h-curves are plotted by choosing h_1, h_2 and h_3 in such a manner that the solutions (31)–(33) ensure convergence [28]. Here to see the admissible values of h_1, h_2 and h_3, the h-curves are plotted for 15th-order of approximation in Figs. 1–3 by taking the values of the parameters $Pr = 0.71$, $Gr = 10$, $r_T = 0.5$, $R = 2$, $Re = 2$, $\beta_h = 2$, $\beta_i = 2$, $\alpha = 1$, $Ha = 2$, $Br = 0.5$ and $A = 1$. It is clearly noted from Fig. 1 that the range for the admissible values of h_1 is $-1.25 < h_1 < -0.25$. From Fig. 2, it can be seen that the

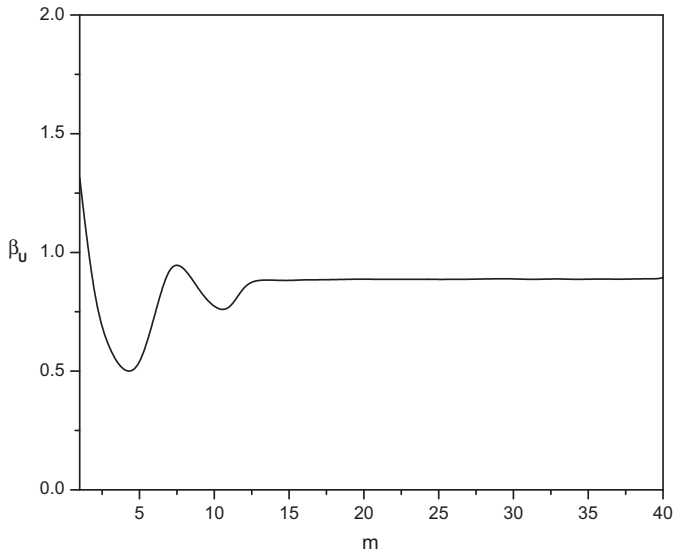

Fig. 7. The ratio β_U from the theorem to reveal the convergence of the HAM solutions.

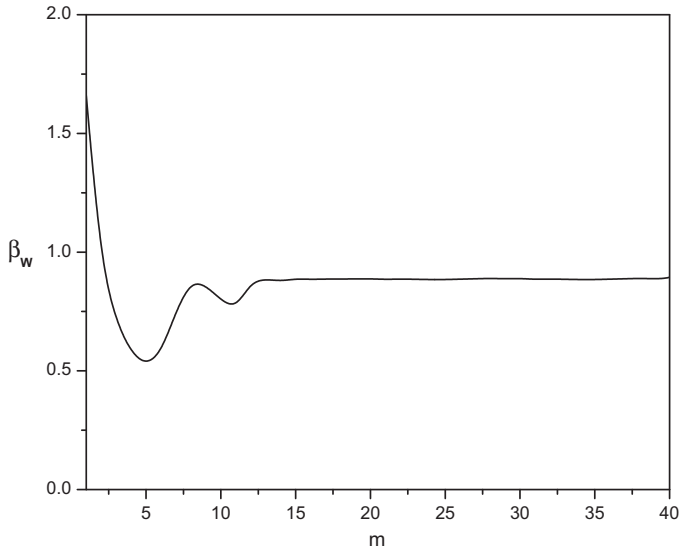

Fig. 8. The ratio β_W from the theorem to reveal the convergence of the HAM solutions.

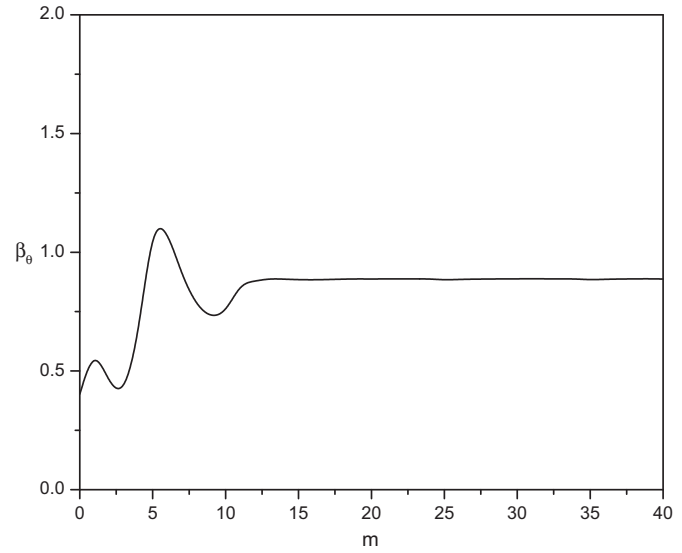

Fig. 9. The ratio β_θ from the theorem to reveal the convergence of the HAM solutions.

h-curve has a parallel line segment that corresponds to a region $-1.2 < h_2 < -0.4$. Fig. 3 depicts that the admissible value of h_3 are $-1.5 < h_3 < -0.5$. A wide valid zone is evident in these figures ensuring convergence of the series. To choose optimal value of auxiliary parameter, the average residual errors (see Ref. [30] for more details) are defined as

$$E_{U,m} = \frac{1}{2K}\sum_{i=-K}^{K}\left(N_1\left[\sum_{j=0}^{m} U_j(i\triangle t)\right]\right)^2, \tag{37}$$

$$E_{W,m} = \frac{1}{2K}\sum_{i=-K}^{K}\left(N_2\left[\sum_{j=0}^{m} W_j(i\triangle t)\right]\right)^2, \tag{38}$$

$$E_{\theta,m} = \frac{1}{2K}\sum_{i=-K}^{K}\left(N_3\left[\sum_{j=0}^{m} \theta_j(i\triangle t)\right]\right)^2, \tag{39}$$

Table 5
Comparison of flow velocity (U) for $Ha = R = Gr/Re = 0$.

	$\alpha = 0.5$		$\alpha = 0.75$		$\alpha = 1$	
η	Analytical	HAM	Analytical	HAM	Analytical	HAM
−1	0	0	0	0	0	0
−0.5	0.227539	0.227539	0.153714	0.153714	0.105763	0.105763
0	0.316451	0.316451	0.21478	0.21478	0.148054	0.148054
0.5	0.227539	0.227539	0.153714	0.153714	0.105763	0.105763
−1	0	0	0	0	0	0

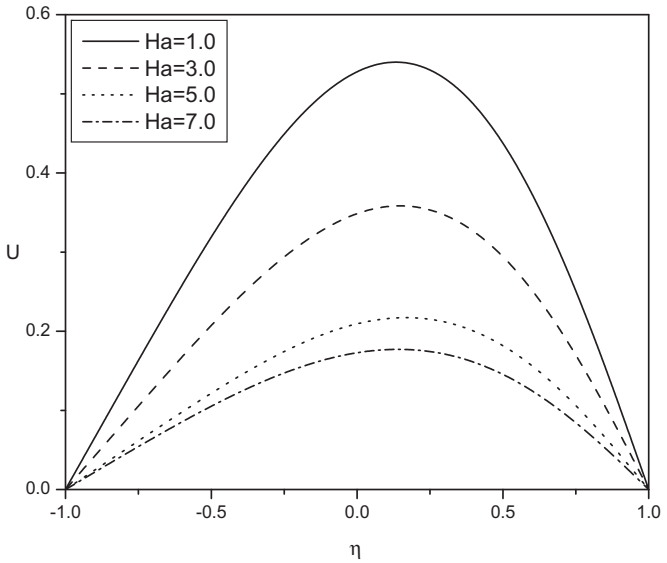

Fig. 10. Magnetic effect (Ha) on U at $\beta_h = 2.0$, $\beta_i = 2.0$, $h = -1$, $\alpha = 0.5$.

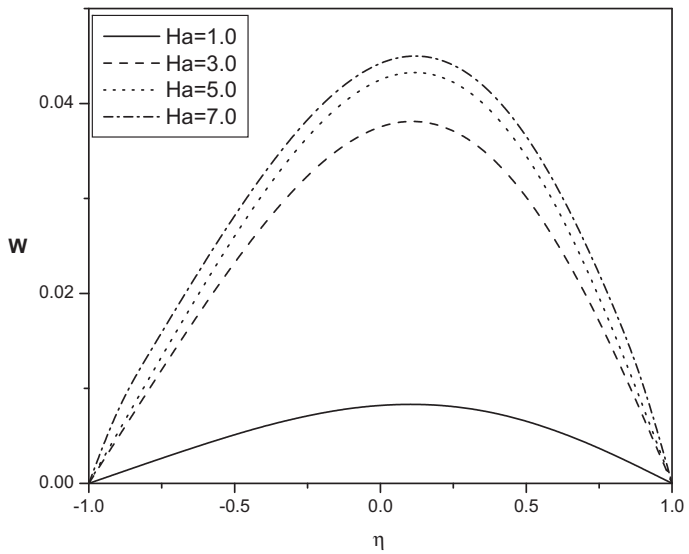

Fig. 11. Magnetic effect (Ha) on W at $\beta_h = 2.0$, $\beta_i = 2.0$, $h = -1$, $\alpha = 0.5$.

where $\triangle t = 1/K$ and K = 5. At different order of approximations (m), minimum of average residual errors are shown in Tables 1–3. It is clear from Table 1 that the average residual error for U is minimum at $h_1 = -1.02$. It can be seen from Table 2 that

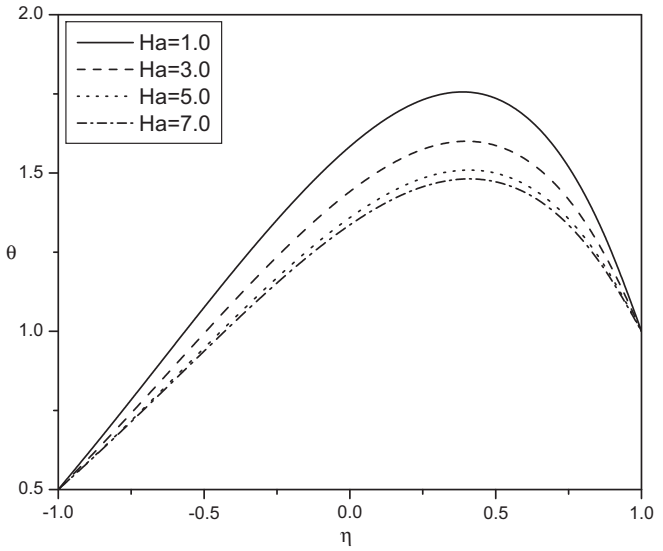

Fig. 12. Magnetic effect (Ha) on θ at $\beta_h = 2.0$, $\beta_i = 2.0$, $h = -1$, $\alpha = 0.5$.

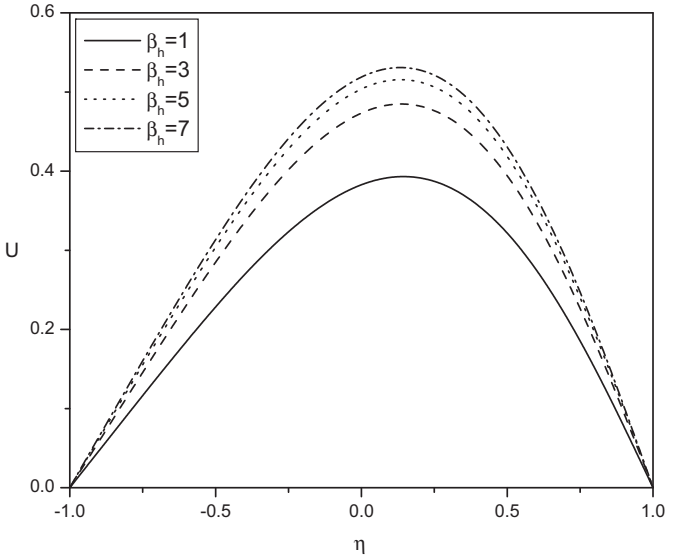

Fig. 13. Effect of β_h on U at $\beta_i = 2.0$, $h = -1$, $\alpha = 0.5$, $Ha = 5$.

the minimum of average residual error for W attains at $h_2 = -0.99$. Table 3 depicts that at $h_3 = -0.98$, E_θ attains minimum. Therefore, the optimum values of convergence control parameters are taken as $h_1 = -1.02$, $h_2 = -0.99$, $h_3 = -0.98$.

To see the accuracy of the solutions, the residual errors are defined for the system as

$$RE_U = \alpha^2 U_n^{(iv)} - U_n'' + RU_n' - \frac{Gr}{Re}\theta_n + \frac{Ha^2}{\alpha_e^2 + \beta_h^2}(\alpha_e U_n + \beta_h W_n) + A, \tag{40}$$

$$RE_W = \alpha^2 W_n^{(iv)} - W_n'' + RW_n' - \frac{Ha^2}{\alpha_e^2 + \beta_h^2}(\beta_h U_n - \alpha_e W_n), \tag{41}$$

$$RE_\theta = \theta_n'' - RPr\theta_n' + \gamma_1 RPr\theta_n + 2Br[(U_n')^2 + (W_n')^2] + \alpha^2 Br[(U_n'')^2 + (W_n'')^2], \tag{42}$$

where $U_n(\eta)$, $W_n(\eta)$ and $\theta_n(\eta)$ are the HAM solution for $U(\eta)$, $W(\eta)$ and $\theta(\eta)$. For optimality of the convergence control parameters, residual error [31] for different values of h in the convergence region displayed in Figs. 4–6. We examine that $h_1 = -1.02$, $h_2 = -0.99$, $h_3 = -0.98$ gives a better solution. Table 4 establishes the convergence of the obtained series solution.

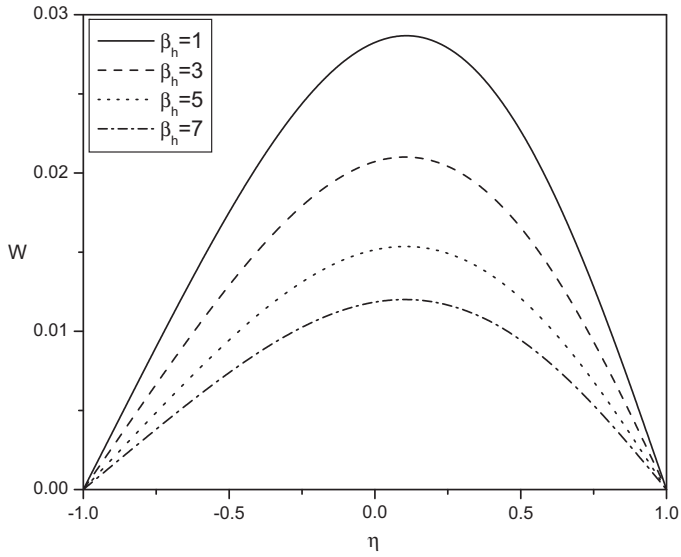

Fig. 14. Effect of β_h on W at $\beta_i = 2.0$, $h = -1$, $\alpha = 0.5$, $Ha = 5$.

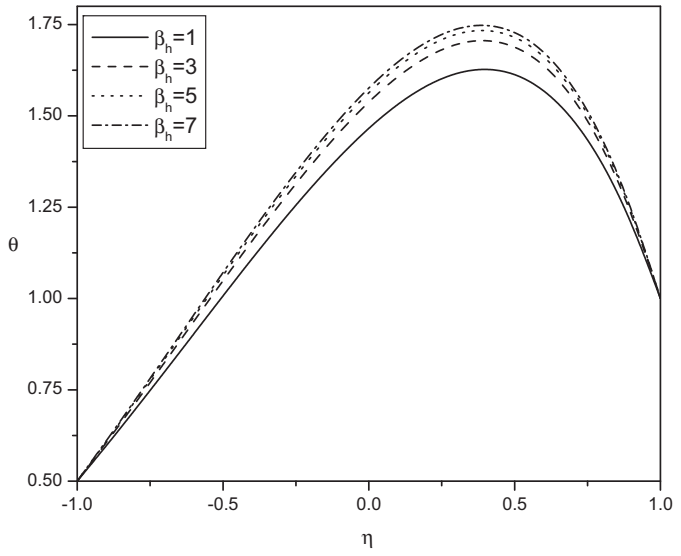

Fig. 15. Effect of β_h on θ at $\beta_i = 2.0$, $h = -1$, $\alpha = 0.5$, $Ha = 5$.

It is found from the above observations that the series given by (31)–(33) converge in the whole region of η when $h_1 = -1.02$, $h_2 = -0.99$, $h_3 = -0.98$.

In order to pursue the convergence of the HAM solutions to the exact ones, the graphs for the ratio (following the recent work of [34])

$$\beta_U = \left|\frac{U_m(h)}{U_{m-1}(h)}\right|, \quad \beta_W = \left|\frac{W_m(h)}{W_{m-1}(h)}\right|, \quad \beta_\theta = \left|\frac{\theta_m(h)}{\theta_{m-1}(h)}\right| \tag{43}$$

against the number of terms m in the homotopy series is presented in Figs. 7–9. Figures strongly indicate that a finite limit of β will be attained in the limit of $m \to \infty$, which will remain less than unity (actually figures imply a limit of 0.88 for U, W and θ). The velocity and temperature solutions seem to converge in an oscillatory manner requiring more terms in the homotopy series. Thus, the convergence to the exact solution is assured by the HAM method.

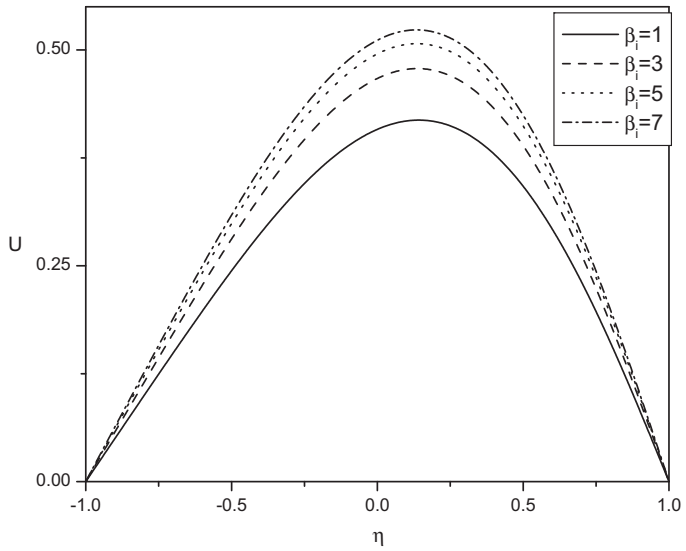

Fig. 16. Effect of β_i on U at $\beta_h = 2.0$, $h = -1$, $\alpha = 0.5$, $Ha = 5$.

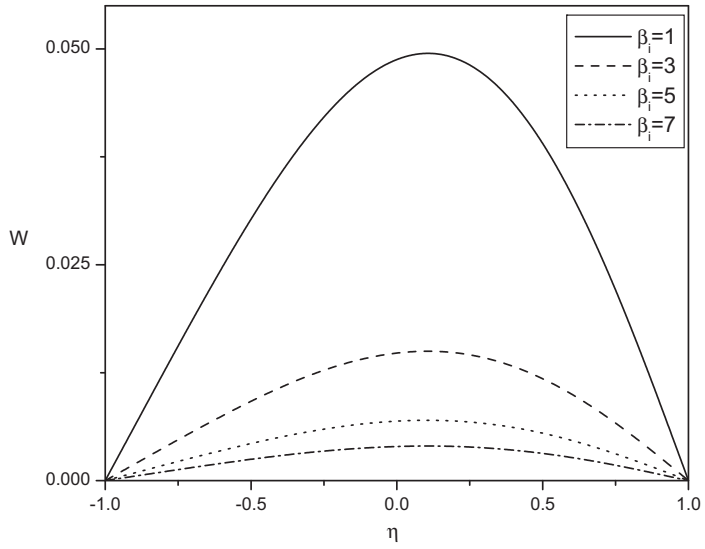

Fig. 17. Effect of β_i on W at $h = -1$, $\alpha = 0.5$, $Ha = 5$.

5. Results and discussion

In the absence of Hartmann number Ha, suction/injuction parameter R and Buoyancy ratio Gr/Re, Eq. (7) reduces to the equation of motion for the flow between parallel plates given in text book by Stokes ([26], page no. 44). Analytical solution of that equation with type A conditions and HAM solution at different α are shown in Table 5. The comparisons are found to be in a very good agreement. Therefore, the HAM code can be used with great confidence to study the problem considered in this paper.

The solutions for $U(\eta)$, $W(\eta)$ and $\theta(\eta)$ have been computed and shown graphically in Figs. 10–21. The effects of magnetic parameter (Ha), Hall parameter (β_h), Ion-slip parameter (β_i) and couple stress fluid parameter (α) have been discussed. To study the effect of Ha, β_h, β_i and α, computations were carried out by taking $Pr = 0.73$, $Gr = 10$, $r_T = 0.5$, $R = 2$, $Re = 2$, $Br = 0.5$ and $A = 1$.

Fig. 10 displays the effect of the magnetic parameter Ha on $U(\eta)$. It can be observed that the velocity $U(\eta)$ decreases with an increase in the parameter Ha. This is due to the fact that, the introduction of a transverse magnetic field, normal to the flow direction, has a tendency to create the drag known as the Lorentz force which tends to resist the flow. Hence the

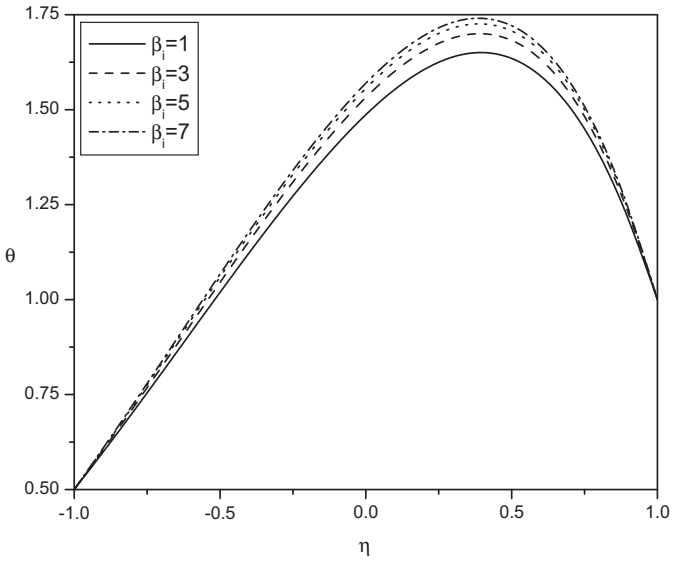

Fig. 18. Effect of β_i on θ at $\beta_h = 2.0$, $h = -1$, $\alpha = 0.5$, $Ha = 5$.

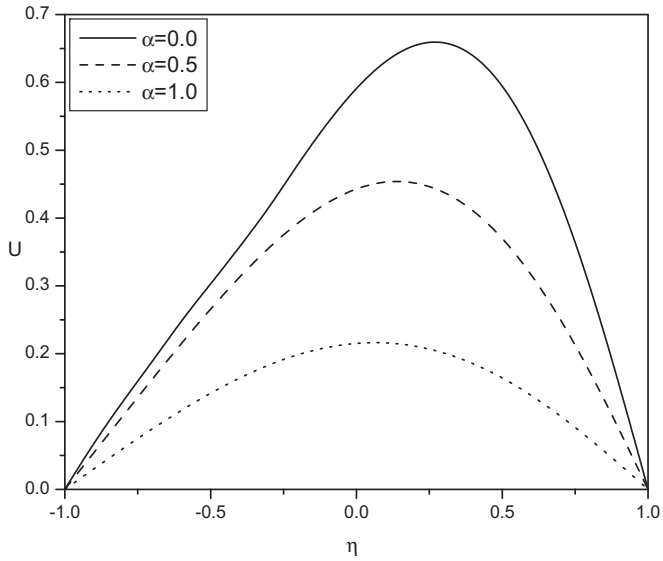

Fig. 19. α Effect on U at $\beta_h = 2.0$, $\beta_i = 2.0$, $h = -1$, $Ha = 5$.

velocity decrease as the magnetic parameter Ha increases. The effect of Ha on the induced flow in z-direction $W(\eta)$ is shown in Fig. 11. It can be seen from this figure that $W(\eta)$ increases with an increase in the parameter Ha. Fig. 12 depicts the variation of temperature with Ha. The temperature $\theta(\eta)$ decreases with an increase in the parameter Ha. As explained above, the transverse magnetic field gives rise to a resistive force known as the Lorentz force of an electrically conducting fluid. This force makes the fluid experience a resistance by increasing the friction between its layers and thus decreases its temperature and concentration.

The variation of velocity components $U(\eta)$ and $W(\eta)$ and temperature $\theta(\eta)$ with β_h is shown in Figs. 13–15. We see that the dimensionless velocity component $U(\eta)$ and temperature $\theta(\eta)$ increase with an increase in the parameter β_h. The inclusion of Hall parameter decreases the resistive force imposed by the magnetic field due to its effect in reducing the effective conductivity. Hence, the velocity component $U(\eta)$ and temperature $\theta(\eta)$ increases as the Hall parameter increases. The induced flow in the z-direction decreases as β_h increases.

Figs. 16–18 represent the effect of the Ion-slip parameter β_i on $U(\eta)$, $W(\eta)$ and $\theta(\eta)$. It can be seen from these figures that the velocity $U(\eta)$ increase with an increase in the parameter β_i. The induced flow in the z-direction decreases with an

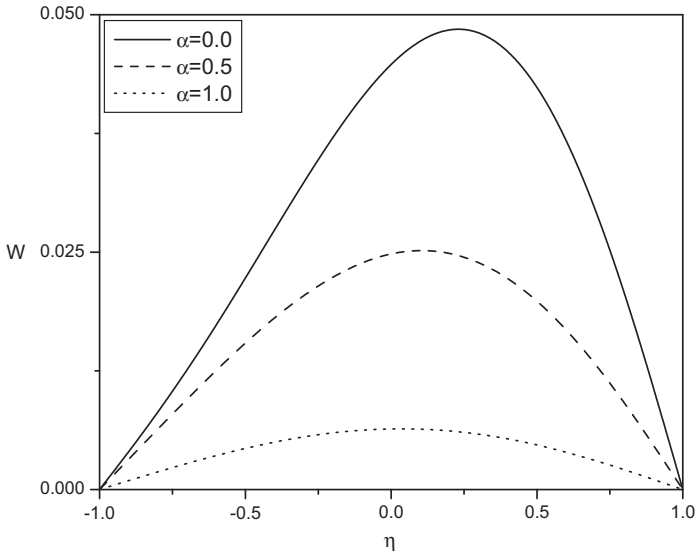

Fig. 20. α Effect on W at $\beta_h = 2.0$, $\beta_i = 2.0$, $h = -1$, $Ha = 5$.

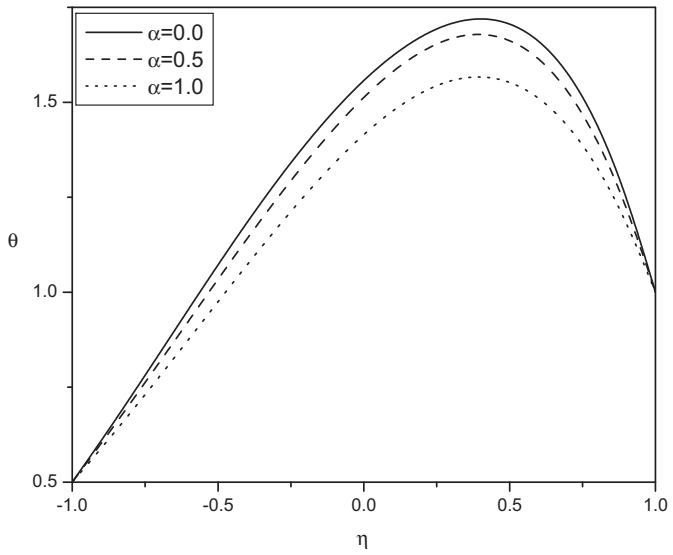

Fig. 21. α Effect on θ at $\beta_h = 2.0$, $\beta_i = 2.0$, $h = -1$, $Ha = 5$.

increase in the parameter β_i. The temperature $\theta(\eta)$ increases with an increase in parameter β_i. As β_i increases the effective conductivity also increases, in turn, decreases the damping force on the velocity component in the direction of the flow, and hence the velocity component in the flow direction increases.

Figs. 19–21 indicate the effect of the Couple stress fluid parameter α on $U(\eta)$, $W(\eta)$ and $\theta(\eta)$. As the couple stress fluid parameter α increases, the velocity $U(\eta)$, the induced flow in the z-direction $W(\eta)$ decrease. It is also clear that the temperature $\theta(\eta)$ decreases with an increase in α. It can be noted that the velocity in case of couple stress fluid is less than that of a Newtonian fluid case. Thus, the presence of couple stresses in the fluid decreases the velocity and temperature.

6. Conclusions

In this paper, the Hall and Ion-slip effects on fully developed electrically conducting couple stress fluid flow between vertical parallel plates has been studied. The governing equations are expressed in the non-dimensional form and are solved by using HAM. The features of flow characteristics are analyzed by plotting graphs and discussed in detail. The main findings are summarized as follows:

- As the magnetic parameter increases, velocity in the direction of the flow and the temperature are decreased and the induced flow velocity component is increased.
- The velocity in the flow direction and temperature are increasing and the induced flow in the z-direction is decreasing as the Hall parameter increases.
- The velocity in the flow direction and the temperature increase and induced flow in the z-direction decreases with an increase in the Ion slip parameter.
- It is noticed that the presence of couple stresses in the fluid decreases the velocity and temperature.

References

[1] Aung W, Worku G. Theory of fully developed, combined convection including flow reversal. J Heat Transfer 1986;108:485–8.
[2] Cheng CH, Kou HS, Huang WH. Flow reversal and heat transfer of fully developed mixed convection in vertical channels. J Thermophys 1990;3:375–83.
[3] Boulama K, Galanis N. Analytical solution for fully developed mixed convection between parallel vertical plates with heat and mass transfer. J Heat Transfer 2004;126:381–8.
[4] Rao, Madhusudhana G, Narasimham GSVL. Laminar conjugate mixed convection in a vertical channel with heat generating components. Int J Heat Mass Transfer 2007;50:3561–74.
[5] Ameni Mokni, Hatem Mhiri, Georges Le Palec, Philippe Bournot. Mixed convection in a vertical heated channel: influence of the aspect ratio. Int J Eng Appl Sci 2009;5(1):60–6.
[6] Alireza S, Sahai V. Heat transfer in developing magnetohydrodynamic Poiseuille flow and variable transport properties. Int J Heat Mass Transfer 1990;33:1711–20.
[7] Umavathi JC, Malashetty MS. Magnetohydrodynamic mixed convection in a vertical channel. Int J Non-Linear Mech 2005;40:91–101.
[8] Barletta A, Cellia M. Mixed convection MHD flow in a vertical channel: effects of Joule heating and viscous dissipation. Int J Heat Mass Transfer 2008;51:6110–7.
[9] Prathapkumar J, Umavathi JC, Biradar BM. Mixed convection of composite porous medium in a vertical channel with asymmetric wall heating conditions. J Porous Medium 2010;13:271–85.
[10] Tani I. Steady flow of conducting fluids in channels under transverse magnetic fields with consideration of Hall effects. J Aerospace Sci 1962;29:297–305.
[11] Sondalgekar VM, Vighnesam NV, Takhar HS. Hall and Ion-slip effects in MHD Couette flow with heat trasfer. IEEE Trans Plasma Sci 1979;7:178–82.
[12] Attia HA. Unsteady couette flow with heat transfer considering Ion slip. Turk J Phys 2005;29:379–88.
[13] Ali J, Chamkha T. Grosan and Ioan Pop, fully developed mixed convection of a micropolar fluid in a vertical channel. Int J Fluid Mech Res 2003;30:1–13.
[14] Ziabakhsh Z, Domairry G. Analytic solution of natural convection flow of a non-Newtonian fluid between two vertical flat plates using homotopy analysis method. Commun Nonlinear Sci Numer Simul 2009;14:1868–80.
[15] Sajid M, Pop I, Hayat T. Fully developed mixed convection flow of a viscoelastic fluid between permeable parallel vertical plates. Comput Math Appl 2010;59:493–8.
[16] Brian S. Energy stability in the Bnard problem for a fluid of second grade. Zeitschrift fr Angewandte Mathematik und Physik (ZAMP). 1983;34(4):502–9.
[17] Kaloni PN, Siddiqui AM. The flow of a second grade fluid. Int J Eng Sci 1983;21(10):1157–69.
[18] Rudraiah N, Radhadevi PV, Kaloni PN. Convection in a viscoelastic fluid saturated sparsely packed porous layer. Canadian J Phys 1990;68:1446–53.
[19] Kaloni PN, Lou JX. Nonlinear convection of a viscoelastic fluid with inclined temperature gradient. Continuum Mech. Thermodynam. 2005;17:17–27.
[20] Hayat T, Ellahi R, Mahomed FM. Exact solution of a thin film flow of an Oldroyd 6-constant fluid over a moving belt. Commun Nonlinear Sci Numer Simul 2009;14(1):133–9.
[21] Ahmad I, Sajid M, Hayat T. Heat transfer in unsteady axisymmetric second grade fluid. Appl Math Comput 2009;215(5):1685–95.
[22] Ellahi R, Hayat T, Mahomed FM, Zeeshan A. Exact solutions for flows of an Oldroyd 8-constant fluid with nonlinear slip conditions. Commun Nonlinear Sci Numer Simul 2010;15(2):322–30.
[23] Vieru D, Fetecau C, Athar M, Fetecau C. Flow of a generalized Maxwell fluid induced by a constantly accelerating plate between two side walls. Zeitschrift Fr Angewandte Mathematik Und Physik (Zamp) 2009;60(2):334–43.
[24] Khan M, Sidra Mahmood, Fetecau C. New exact solutions for magnetohydrodynamic flows of an Oldroyd-B fluid. Zeitschrift Fr Angewandte Mathematik Und Physik (Zamp) 2009;60(6):1206–19.
[25] Fetecau C, Vieru D, Mahmood A, Fetecau C. On the energetic balance for the flow of a Maxwell fluid due to a constantly accelerating plate. Acta Mech 2009;203:89–96.
[26] Stokes VK. Couple Stresses in fluid. Phys Fluids 1966:1709–15.
[27] Stokes VK. Theories of fluids with microstructure: an introduction. New York: Springer Verlag; 1984.
[28] Liao SJ. Beyond perturbation. Introduction to homotopy analysis method. Boca Raton: Chapman and Hall/CRC Press; 2003.
[29] Liao SJ. On the homotopy analysis method for nonlinear problems. Appl Math Comput 2004;147(2):499–513.
[30] Liao SJ. An optimal homotopy-analysis approach for strongly nonlinear differential equations. Commun Nonlinear Sci Numer Simul 2010;15:2003–16.
[31] Rashidi MM, Mohimanian pour SA, Abbasbandy S. Analytic approximate solutions for heat transfer of a micropolar fluid through a porous medium with radiation. Commun Nonlinear Sci Numer Simul 2011;16:1874–89.
[32] Si Xin-Hui, Zheng Lian-Cun, Zhang Xin-Xin, Chao Ying. Homotopy analysis solutions for the asymmetric laminar flow in a porous channel with expanding or contracting walls. Acta Mech Sin 2011;27(2):208–14.
[33] Turkyilmazoglu M. Some issues on HPM and HAM methods: a convergence scheme. Math Comput Model 2011;53:1929–36.
[34] Turkyilmazoglu M. Numerical and analytical solutions for the flow and heat transfer near the equator of an MHD boundary layer over a porous rotating sphere. Int J Thermal Sci 2011;50:831–42.